Published OnlineFirst May 8, 2017; DOI: 10.1158/1541-7786.MCR-16-0424

Oncogenes and Tumor Suppressors

Molecular Cancer Research

Regulation of *USP37* Expression by REST-Associated G9a-Dependent Histone Methylation

Tara H.W. Dobson[1], Rashieda J. Hatcher[1], Jyothishmathi Swaminathan[1], Chandra M. Das[1], Shavali Shaik[1], Rong-Hua Tao[1], Ciro Milite[2], Sabrina Castellano[2], Pete H. Taylor[1], Gianluca Sbardella[2], and Vidya Gopalakrishnan[1,3,4,5,6]

Abstract

The deubiquitylase (DUB) USP37 is a component of the ubiquitin system and controls cell proliferation by regulating the stability of the cyclin-dependent kinase inhibitor 1B, (CDKN1B/p27Kip1). The expression of USP37 is downregulated in human medulloblastoma tumor specimens. In the current study, we show that USP37 prevents medulloblastoma growth in mouse orthotopic models, suggesting that it has tumor-suppressive properties in this neural cancer. Here, we also report on the mechanism underlying *USP37* loss in medulloblastoma. Previously, we observed that the expression of *USP37* is transcriptionally repressed by the *RE1* silencing transcription factor (REST), which requires chromatin remodeling factors for its activity. Genetic and pharmacologic approaches were employed to identify a specific role for G9a, a histone methyltransferase (HMT), in promoting methylation of histone H3 lysine-9 (H3K9) mono- and dimethylation, and surprisingly trimethylation, at the *USP37* promoter to repress its gene expression. G9a inhibition also blocked the tumorigenic potential of medulloblastoma cells *in vivo*. Using isogenic low- and high-REST medulloblastoma cells, we further showed a REST-dependent elevation in G9a activity, which further increased mono- and trimethylation of histone H3K9, accompanied by downregulation of *USP37* expression. Together, these findings reveal a role for REST-associated G9a and histone H3K9 methylation in the repression of *USP37* expression in medulloblastoma.

Implications: Reactivation of USP37 by G9a inhibition has the potential for therapeutic applications in REST-expressing medulloblastomas. *Mol Cancer Res; 15(8); 1073–84. ©2017 AACR.*

Introduction

Medulloblastoma is a malignant pediatric brain tumor. It frequently arises in the cerebellum and is characterized by poor neuronal differentiation and hyperproliferation (1–3). Current therapies, although efficacious against primary tumors, cause severe neurologic deficits in children with brain tumors (4). Therapies targeting tumor-specific molecular events are needed to minimize treatment-related toxicities (4).

The *RE1* silencing transcription factor (REST), a repressor of neuronal specification, has been implicated in medulloblastoma development. Its expression is elevated in human medulloblastoma samples and is associated with poor prognostic significance for patients (5–7). Previous work showed that REST knockdown in human medulloblastoma cells abrogated its tumorigenic potential in murine orthotopic models, suggesting that it is required for tumor maintenance (8). REST is also coexpressed with c-Myc or N-Myc in human medulloblastoma samples and cooverexpression of REST and v-Myc in mouse neural progenitors promoted cerebellar tumors that resembled human medulloblastomas (6). These observations are consistent with a function for REST in tumor progression. Finally, REST-positive tumors were poorly differentiated, which is in agreement with its known function as a repressor of neuronal differentiation genes (9–11).

In more recent studies, we observed that REST elevation also contributed to deregulation of medulloblastoma cell proliferation (7, 12). We determined that REST-dependent maintenance of tumor cell proliferation was mediated by an ubiquitin-specific protease (USP) called USP37, which we identified as a novel transcriptional target of REST's repressive activity (5). USP37 is a member of the USP family of deubiquitylases (DUB) and is one of a large number of DUBs that have been described in the literature based on sequence comparison (13–17). DUBs are enzymes that catalyze the proteolytic removal of ubiquitin moieties from proteins and oppose the coordinated activities of ubiquitin-activating enzyme E1, ubiquitin-conjugating enzyme E2, and ubiquitin ligase E3, which catalyze the addition of ubiquitin residues

[1]Department of Pediatrics, University of Texas, MD Anderson Cancer Center, Houston, Texas. [2]Epigenetic Medicinal Chemistry Lab, Dipartimento di Farmacia, Università degli Studi di Salerno, Fisciano (SA), Italy. [3]Department of Molecular and Cellular Oncology, University of Texas, MD Anderson Cancer Center, Houston, Texas. [4]Center for Cancer Epigenetics, University of Texas, MD Anderson Cancer Center, Houston, Texas. [5]Brain Tumor Center, University of Texas, MD Anderson Cancer Center, Houston, Texas. [6]Program in Neuroscience, The University of Texas Graduate School of Biomedical Sciences, Houston, Texas.

Note: Supplementary data for this article are available at Molecular Cancer Research Online (http://mcr.aacrjournals.org/).

T.H.W. Dobson, R.J. Hatcher, and J. Swaminathan contributed equally to this article.

Corresponding Author: Vidya Gopalakrishnan, The University of Texas MD Anderson Cancer Center, 1515 Holcombe Boulevard, Unit 853, Houston, TX 77030. Phone: 713-792-0498; Fax: 713-563-5407: E-mail: vgopalak@mdanderson.org

doi: 10.1158/1541-7786.MCR-16-0424

Published OnlineFirst May 8, 2017; DOI: 10.1158/1541-7786.MCR-16-0424

to proteins (18, 19). Thus, these two processes maintain cellular homeostasis and are perturbed in a number of cancers (20). Because ubiquitylation is a reversible process and can be targeted pharmacologically, DUBs are also gaining traction as druggable targets for cancer (13, 21).

We had previously shown that USP37 is required for the stabilization of the cyclin-dependent kinase inhibitor (CDKI), p27 (5). The failure to stabilize p27 in REST-high and USP37-low medulloblastoma cell lines was shown to directly promote deregulated cell proliferation (5). However, the requirement for USP37 in medulloblastoma growth *in vivo* and the specific mechanism(s) utilized by the REST complex in repressing USP37 in tumor cells are not known. Here, we demonstrate that constitutive USP37 expression suppresses medulloblastoma growth in mouse orthotopic models. We also provide genetic and pharmacologic evidence in support of a role for the HMT G9a and histone H3K9 methylation in silencing *USP37* expression and show that pharmacologic inhibition of G9a blocks the growth of medulloblastoma cells *in vitro* and suppresses their tumorigenic potential *in vivo*. Finally, using isogenic low-REST and high-REST medulloblastoma cell lines, we show that G9a promotes repression of *USP37* expression in a REST-dependent manner. Thus, our findings not only suggest a tumor-suppressive role for USP37 in medulloblastoma development, but also provide data to support the further exploration of G9a inhibitors for therapeutic intervention in REST-positive medulloblastomas.

Materials and Methods

Cell culture/transfections

DAOY (ATCC), DAOY-REST, D283, and UW426 were cultivated as described previously (7). Cell identity was confirmed using short tandem repeat fingerprinting (Characterized Cell Line Core, MD Anderson Cancer Center, Houston, TX). Mycoplasma testing was performed every 6 months using MycoAlert Mycoplasma Detection Kit (Lonza). Cells were passaged at least twice after thawing prior to experiments. All experiments were performed within 2 to 3 weeks after cells were thawed and passaged no more than 10 times.

Ectopic expression of mutant G9a was achieved by transient transfection of 2 μg of plasmid pcDNA3.1(+)-G9aH1113K (a gift from Dr. Xiaobing Shi, Department of Epigenetics and Molecular Carcinogenesis, The University of Texas MD Anderson Cancer Center, Houston, TX) or vector alone using Lipofectamine 2000 Reagent (Thermo Fisher Scientific). Cells were harvested after 24 hours and processed for RNA and protein analyses.

MTT assay

E67 was synthesized in accordance with the methods described by Chang and colleagues (22). UNC 0638 was purchased from the Cayman Chemical Company (23). Both drugs were dissolved in DMSO and stored at −20°C. DAOY, DAOY-REST cells (3×10^4), UW426 (4×10^4), and D283 (7.5×10^4) were seeded at the indicated densities in 96-well plates containing 100 μL of media. After overnight incubation, cells were treated for 24, 48, and 72 hours with E67, UNC 0638, or DMSO at concentrations ranging from 0.125 to 10 μmol/L and 0.125 to 4 μmol/L, respectively. MTT assays were performed as described previously (5, 7, 24). Absorbance at 570 nm and background at 650 nm were read on a multiwell spectrophotometer. Results were expressed as a percentage (%) of the control (DMSO).

Live cell nuclear staining assay

DAOY or DAOY-REST cells were seeded at a density of 90,000 cells/well in 6-well plates and incubated overnight. Cells were treated with their respective 48-hour IC_{50} concentrations of UNC 0638 (1.1 and 2.5 μmol/L) in a final volume of 3 mL media, incubated for 12, 24, or 48 hours, prior to harvesting for analysis by live cell nuclear staining assay. Cells (1×10^5) were resuspended in 200 μL PBS and were incubated with 2 μL of DRAQ5 for 3 minutes at 37°C and then 5 to 10 minutes at room temperature. Flow cytometry was performed using a FACSCalibur (Becton Dickinson).

qRT-PCR analyses

DAOY, D283, and/or UW426 cells were treated with either 5 μmol/L SAHA (Cayman Chemical Company) for 6, 12, and 24 hours, or 2.5 μmol/L MS-275 (Enzo Life Sciences) for 6, 16, and 24 hours, or 1.1 μmol/L UNC 0638 (IC_{25} at 48 hours) for 4 or 12 hours. Cells were harvested for RNA extraction using Quick RNA Kit (Genesee Scientific). RNA recovery and purity were determined by NanoDrop Spectrophotometer ND-1000 (Thermo Fisher Scientific). cDNA libraries were synthesized using iScript cDNA Synthesis Kit (Bio-Rad), and qRT-PCR was performed using Roche Lightcycler 96 (Roche) according to the manufacturer's instructions. For primers, see Supplementary Data.

Chromatin immunoprecipitation assays

DAOY or DAOY-REST cells were treated with 1.1 μmol/L UNC 0638 or DMSO for 12 hours prior to fixation, cross-linking, and processing for chromatin immunoprecipitation (ChIP) analyses as described previously (5). Cross-linked cells were resuspended in sonication buffer [50 mmol/L Tris-HCl (pH 8.0), 10 mmol/L EDTA (pH 8.0), 1% SDS, and protease inhibitors] and sonicated, and 10% of this material was saved as input DNA. The remainder of the samples was diluted 5-fold with ChIP dilution buffer [16.7 mmol/L Tris-HCl (pH 8.0), 167 mmol/L NaCl, 1.2 mmol/L EDTA (pH 8.0), 1.1% Triton X-100, and protease inhibitors], precleared, and incubated with various antibodies for 12 hours at 4°C. Following incubation with protein-A beads, washing, and elution, the cross-linking was reversed and DNA was purified with a QiaQuick PCR Purification Kit (Qiagen). Bound DNA was quantified by SYBRGreen qPCR using Roche Lightcycler 96. Data were analyzed using the comparative $2^{-\Delta\Delta Ct}$ method (7). For antibody and primer information, see Supplementary Data.

Western blot analysis

Cells were harvested in RIPA lysis buffer containing a cocktail of protease inhibitors (Thermo Fischer Scientific) and phosphatase inhibitors (Sigma-Aldrich). Equal amount of protein was electrophoresed and subjected to Western blot analyses. For antibody list, see Supplementary Data. Immunoreactive bands were detected using SuperSignal West Dura Extended Duration Substrate (Pierce).

In vivo measurement of tumor growth

All animal experiments were approved by the Institutional Animal Care and Use Committee. Orthotopic cerebellar injections of isogenic DAOY and DAOY-REST cells, pretreated with UNC 0638 (IC_{25} for DAOY cells at 48 hours, 1.1 μmol/L) for 12 hours, were performed using 4- to 6-week-old NOD *scid* gamma null (NSG; NOD.Cg-*Prkdc*^{scid} *Il2rg*^{tm1Wjl}/SzJ JAX) mice (The Jackson Laboratory; ref. 24). Bioluminescence imaging (BLI) was

Published OnlineFirst May 8, 2017; DOI: 10.1158/1541-7786.MCR-16-0424

performed to monitor tumor growth using an IVIS Spectrum (Caliper), following intraperitoneal injection injection of D-luciferin. Data were analyzed using Living Image (Xenogen) software. Mice were sacrificed after 13 days and brains were formalin fixed for histopathology assessment.

IHC

IHC staining was performed on paraffin-embedded brain sections (4 μm). Paraffin-embedded brain sections were deparaffinized, rehydrated, and treated to inactivate the endogenous peroxidase activity. Antigen retrieval was then performed using a pressure cooker (Aroma) using a sodium citrate buffer (10mmol/L, pH 6.0). Samples were washed and blocked in TBS Tween (TBST) containing 1% BSA and 5% normal goat serum. Incubation with primary antibody was then carried out overnight at 4°C. For antibody list, see Supplementary Data. Following incubation with the corresponding secondary antibody, slides were washed with TBST and developed using 3,3′-diaminobenzidine (Vector Laboratories) and counterstained with hematoxylin. Stained slides were viewed using a Nikon ECLIPSE E200 microscope, and images were captured under ×4, ×10, and ×40 magnification with an OLYMPUS SC100 camera.

Results

Constitutive *USP37* expression suppresses medulloblastoma growth

We had previously identified the deubiquitylase *USP37* as a novel target of the transcriptional repressor REST in medulloblastoma cell lines (5). Constitutive USP37 expression in medulloblastoma cells with high REST expression led to stabilization of p27 and cessation of cell proliferation *in vitro*, suggesting that it may have tumor-suppressive properties (5). To test this possibility, *in vivo* experiments were performed wherein DAOY medulloblastoma cells were transiently transfected with a vector expressing *USP37* and injected into the cerebella of immunodeficient mice ($n = 6$). Control animals were injected with cells transfected with vector plasmid. Animals were monitored periodically for signs of morbidity, including head tilt and hemiparesis. All animals were sacrificed at 3 weeks when control mice receiving injections of vector-transfected cells showed signs of morbidity. Brains were harvested and sectioned for tumor analysis. Sections were stained with hematoxylin and eosin (H&E), which revealed a significant reduction in tumor burden in mice receiving injections of DAOY cells expressing *USP37* transgene compared with animals injected with vector-transfected cells (Fig. 1, right). Although tumors where seen in 2 of the 6 mice, the size of tumors was considerably smaller than those in the control group (Fig. 1, left). These observations suggest that USP37 has tumor-suppressive properties.

G9a inhibition blocks medulloblastoma growth *in vitro* and *in vivo*

REST is associated with the mSin3A- histone deacetylase 1/2 (HDAC 1/2) complex at its amino (N) and carboxy (C) termini (25). The carboxy (C) terminus of REST binds to the Co-REST complex, which contains the histone H3K9 HMT-G9a, the histone H3K9 and K4 lysine specific demethylase 1 (LSD1) as well as HDAC1/2 (25) To identify the specific REST-associated activity that is required for regulation of *USP37* expression, REST-expressing human medulloblastoma cells were treated with drugs that target the N- and C-terminal corepressor complexes. We had previously shown that the pan-HDAC inhibitor SAHA (vorinostat) as well as the group 1 HDAC inhibitor MS-275 (entinostat) blocked the growth of medulloblastoma cells *in vitro* and promoted the upregulation of REST target differentiation genes (7). To ask whether HDAC inhibition is sufficient for *USP37* upregulation, DAOY, D283, and UW426 cells were treated with either SAHA or MS-275 for 6 to 24 hours, and *USP37* gene expression was measured by qRT-PCR. As shown in Fig. 2A, treatment of DAOY and D283 cells with SAHA, which promotes REST degradation, resulted in a significant

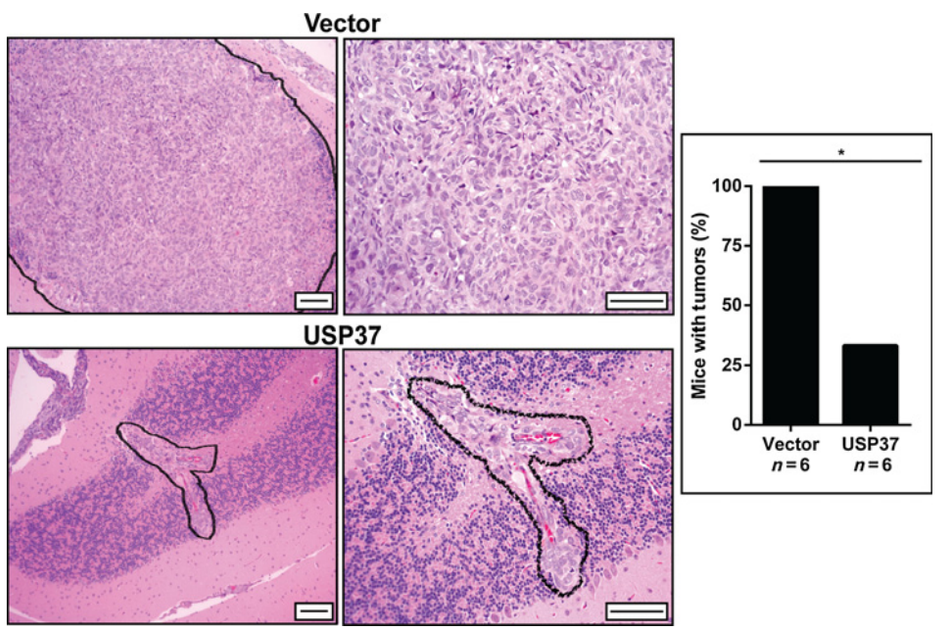

Figure 1.
Constitutive USP37 expression suppresses the growth of medulloblastoma cells in mouse orthotopic models. DAOY cells were transiently transfected with plasmid pDEST26-Flag-HA-USP37 or a vector and implanted into mice cerebella ($n = 6$ each). Animals were sacrificed and brains harvested for H&E staining. Scale bars, 50 μmol/L (left) and 100 μm (right). The bar graph demonstrates the percentage of mice affected with tumor, vector (6/6), and USP37 WT (2/6). Wilcoxon rank sum nonparametric analysis was performed to determine significance (*, $P < 0.05$).

Published OnlineFirst May 8, 2017; DOI: 10.1158/1541-7786.MCR-16-0424

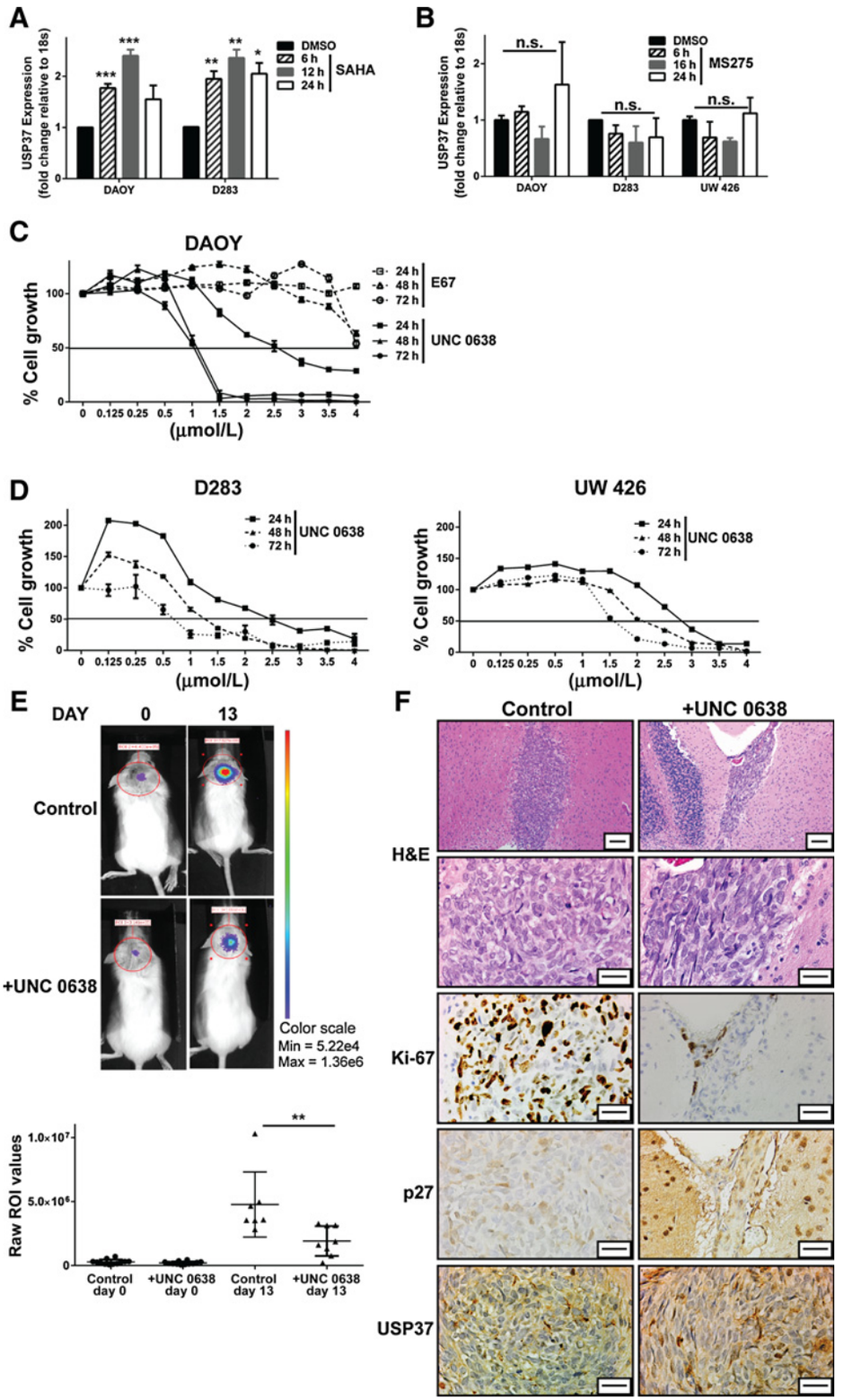

Figure 2.
REST regulates *USP37* expression through H3K9 methylation. **A,** DAOY and D283 cells were treated with 5 μmol/L SAHA (**A**; vorinostat) and DAOY, D283, and UW426 cells were treated with 2.5 μmol/L MS-275 (entinostat) or vehicle (DMSO) for various times followed by qRT-PCR analyses to measure changes in *USP37* gene expression in drug-treated cells compared with untreated cells (**B**). **C,** MTT assays were used to measure the effect of G9a inhibitors E67 and UNC 0638 on mitochondrial activity and cell growth. Solid black line, IC_{50} value, which is also tabulated. **D,** D283 and UW426 cells were treated with UNC 0638 as described in **C**, and MTT assays were performed to obtain IC_{50} values indicated by the dotted line. **E,** DAOY cells stably expressing firefly luciferase were pretreated with 1.1 μmol/L (IC_{50} at 48 hours) for 12 hours and implanted into NSG mice cerebella. Tumor growth was measured by BLI on the day of injection (day 0) and every 4 days thereafter. BLI on days 0 and 13 of representative animals receiving drug-treated (+UNC 0638) and untreated cells (control) is shown (top). Relative flux for the cohort receiving control and drug-treated cells is shown in the bottom graph. **F,** Representative sections obtained from control and UNC 0638–treated cerebellar sections were processed for H&E staining and IHC with antibodies as indicated. Scale bars, 50 μm (top) and 20 μm (bottom). *, $P < 0.05$; **, $P < 0.01$; and ***, $P \leq 0.001$, n.s., not significant).

upregulation of *USP37* gene expression (7). Although MS-275 treatment inhibited REST activity as measured by upregulation of its target neuronal differentiation genes, it did not upregulate *USP37* gene expression (Fig. 2B). These results indicate that targeting HDACs 1/2 activity alone is insufficient to derepress *USP37*.

Table 1. IC_{50} values for G9a inhibitors in DAOY cells

	IC_{50} Values		
Time (hours)	24	48	72
E67 (μmol/L)	7.4	6.5	4.2
UNC 0638 (μmol/L)	2.7	1.1	1.1

As a first step in assessing the involvement of the Co-REST complex in regulating *USP37* expression, the response of DAOY cells to pharmacologic inhibition of G9a was measured as a function of drug concentration and time of exposure to the drug. Treatment of DAOY cells with the G9a inhibitors, E67 and UNC 0638, led to a decline in cell growth as determined by MTT assays (Fig. 2C). Although the entire range of drug concentrations tested for E67 are not shown, a temporal comparison of IC_{50} values (7.4, 6.5, 4.2 versus 2.7, 1.1, and 1.1 μmol/L at 24, 48, and 72 hours, respectively) confirmed that UNC 0638 had a more potent effect on cell growth compared with E67 (Table 1). The decrease in cell growth in response to UNC 0638 treatment was also confirmed in medulloblastoma cell lines with higher (D283) and lower (UW426) REST levels than DAOY cells (Fig. 2D; ref. 7). The effect of G9a inhibition on tumorigenic potential of DAOY cells was also examined in mouse orthotopic models. DAOY cells (50,000/animal, $n = 7$) were treated *ex vivo* with 1.1 μmol/L UNC 0638 (IC_{50} dose at 48 hours) for 12 hours prior to implantation into the cerebellum of immunodeficient NOD/SCID-γ (NSG) animals. A 6.25% decrease in cell viability was expected with these preimplantation treatment parameters. A control group of mice ($n = 8$) was implanted with similar number of cells that were treated with DMSO. Mice were monitored for tumor growth every 4 days by BLI. Animals were sacrificed 13 days after tumor cell implantation when control mice began displaying signs of morbidity. Shown in Fig. 2E (left) are representative images of BLI signals obtained with mice in control (top row) and treatment (bottom row) groups at days 0 and 13. In contrast to the treatment group, a significant increase in bioluminescence intensity was noted within regions of interest in the control cohort at day 13 relative to day 0 (Fig. 2E). H&E staining of brain sections confirmed the decrease in tumor burden in animals receiving UNC 0638–treated cells compared with the control cohort that was seen by BLI analyses (Fig. 2E and F). IHC analyses of brain sections from animals implanted with cells exposed to UNC 0638 also revealed a substantial reduction in Ki-67 positivity, which was associated with an increase in p27 and USP37 staining when compared with the control brains (Fig. 2F). These results suggest that the potential for growth of medulloblastoma cells *in vitro* and *in vivo* can be blocked by G9a inhibition.

G9a represses *USP37* expression by histone H3K9 methylation

As USP37 elevation was seen by IHC following UNC 0638 treatment, we asked whether G9a-dependent histone H3K9 methylation is involved in the regulation of *USP37* gene expression in medulloblastoma cells. First, inhibition of G9a activity following UNC 0638 exposure was studied by Western blotting using lysates of drug or vehicle (DMSO)-treated DAOY cells, which revealed a global decrease in H3K9-me2 and -me3, but not me1 (Fig. 3A). Further confirmation of these results was obtained through qRT-PCR analyses, where a 6.5- to 7.2-fold and 18.1- to 7.4-fold increase was seen in the expression of the known G9a target genes, *NANOG* and *RB*, following exposure of DAOY cells to UNC 0638 for 4 and 12 hours, respectively (Fig. 3B). REST target genes, *TUBB3* (10.1- and 5.9-fold), *SYN1* (5- and 3.3-fold), *SCG10* (11- and 6.6-fold), and *USP37* (5.5- and 3.1-fold) were also upregulated under these conditions, indicating G9a inhibition affected the activity of the REST complex (Fig. 3B).

ChIP assays were next performed to first measure REST binding to the *RE1* consensus sequence in exon 1 of the *USP37*-coding region and then to assess the status of histone H3K9 -me1, -me2, and -me3 within the *USP37* promoter in DAOY cells. qRT-PCR analyses using a pair of primers in the upstream regulatory region of *USP37* proximal to the *RE1* sites showed a 3.4-fold increase in amplification of DNA pulled down by anti-REST antibody relative to control IgG, confirming REST occupancy of the site within exon1 of *USP37* (Fig. 3C). Antibodies specific to histone H3K9 -me1, -me2, and -me3 marks were also used to demonstrate a 190-, 25.7-, and 103.1-fold increase in pull-down of DNA relative to control IgG around position −218 (region-1) and a 238-, 27.6-, and 78.5-fold increase in pull-down of DNA relative to control IgG around position −461 bp (region-2) of the *USP37* promoter (Fig. 3D). Interestingly, UNC 0638 treatment did not alter the levels of histone H3K9-me1 relative to untreated controls at region-1, but did cause a 1.4-fold increase in histone H3K9-me1 at region-2 (Fig. 3D). A 20- and 30-fold decrease in H3K9-trimethylationand a 2- to 2.4-fold increase in histone H3K9-me2 was also observed upon UNC 0638 treatment at regions-1 and -2 of the *USP37* promoter, respectively (Fig. 3D). A role for G9a in the regulation of *USP37* gene expression was also confirmed using genetic approaches. DAOY cells were transfected with the plasmid pcDNA3.1-G9a-H1113K, which expresses a catalytically inactive mutant of G9a with a histidine to lysine change at position 1113 (H1113K) of the protein (26). As shown in Fig. 3E, a global decrease in histone H3K9 -me2 and me3 was seen upon expression of G9a-H1113K mutant, confirming interference with endogenous G9a activity in these cells. A 2.2-fold increase in *USP37* gene expression was observed in cells expressing mutant G9a compared with vector-transfected cells (Fig. 3F). The expression of *SCG10* and *TUBB3* underwent 9.9- and 2,255-fold increases, whereas expression of the G9a target gene, *NANOG*, was elevated 9.9-fold under these conditions (Fig. 3F). Together, the above results validate our hypothesis that *USP37* gene expression is regulated by G9a.

REST-associated G9a activity represses *USP37* gene expression

G9a is associated with a number of chromatin remodeling complexes (27, 28). To assess whether REST-associated G9a regulates *USP37* gene expression, we first asked whether G9a activity was altered in a REST-dependent manner. Western blot analysis of lysates from DAOY cells expressing endogenous REST or human REST transgene (DAOY-REST) showed REST levels to correlate with global increases in histone H3K9 -me1, -me2, and me3 (Fig. 4A). qRT-PCR analyses identified significant decreases in the expression of the REST target genes, *TUBB3*, *SYN1*, *SCG10*, and *USP37* (Fig. 4B). However, expression of the G9a target gene, *NANOG*, was unaffected in REST-high cells, indicating that the effect was specific to REST target genes (Fig. 4B). Consistent with these observations, ChIP experiments revealed a 40.5-fold increase in histone H3K9-me1 and a 36.2-fold increase in histone H3K9-me1 in region-1 of the *USP37* promoter in DAOY-REST cells compared with DAOY cells (Figs. 3C, top and 4C). A smaller 4.7-fold increase in histone H3K9-me1 was noted at region-2 of *USP37* promoter in DAOY-REST cells compared with DAOY cells (Fig. 4C). In addition, growth of DAOY-REST cells was less

Published OnlineFirst May 8, 2017; DOI: 10.1158/1541-7786.MCR-16-0424

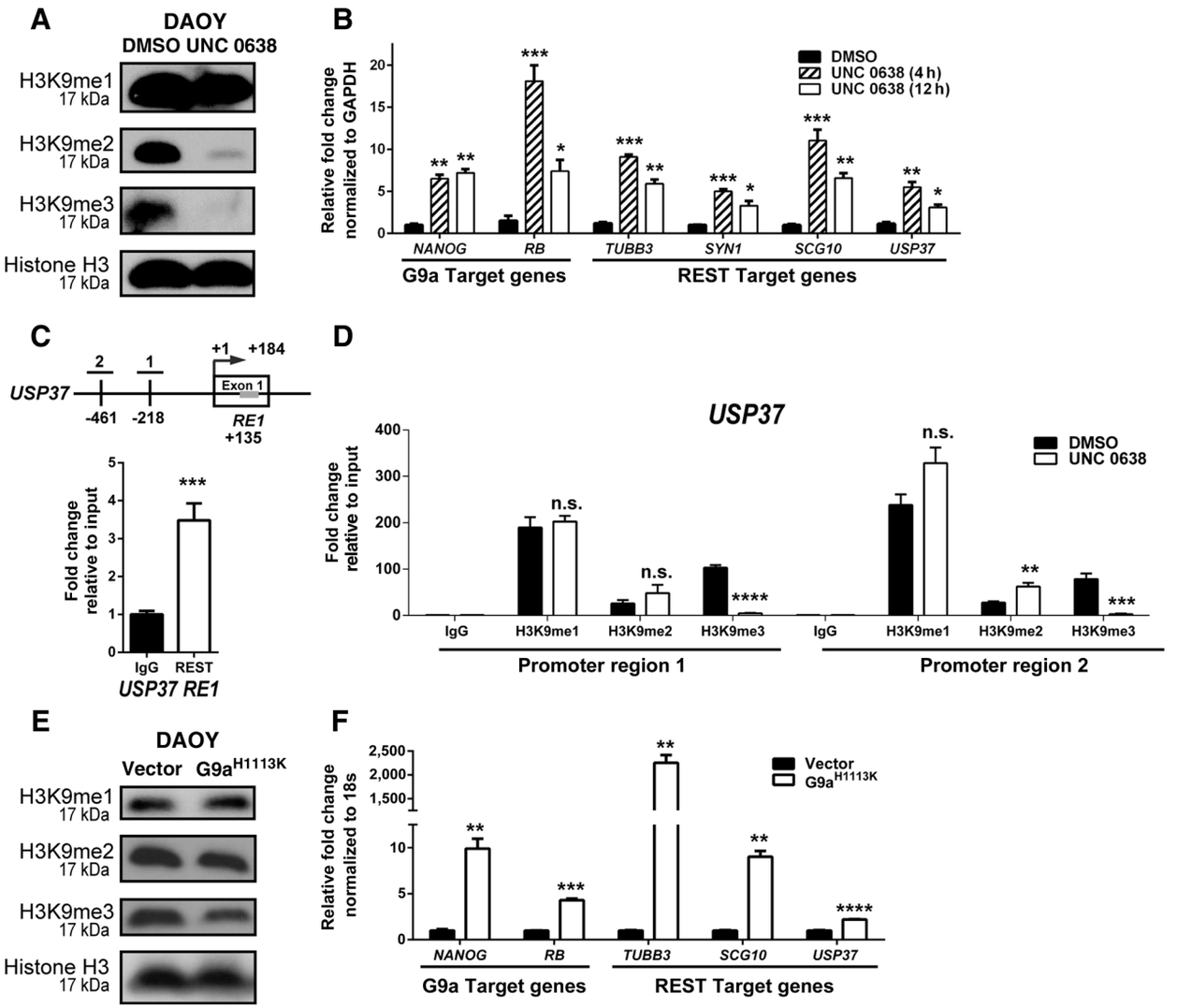

Figure 3.

G9a regulates *USP37* expression. **A,** Western blot analysis was performed with extracts prepared from DAOY cells that were treated with 1.1 μmol/L UNC 0638 or DMSO for 12 hours. Global changes in histone H3K9-me1, -me2, and -me3 were determined. Total histone H3 was used as a loading control. **B,** Changes in the expression of G9a and REST-target genes were established by qRT-PCR analyses following treatment with UNC 0638 for 4 or 12 hours. DMSO-treated cells were used as controls. **C,** Schematic representation of the *USP37* promoter region with locations of the *RE1* site (gray bar, +135 bp), and CpG island proximal region-1 (−218 bp) and region-2 (−461 bp) is shown. Specific REST binding to the *RE1* site (normalized to IgG) was demonstrated by ChIP assay. Data are represented as fold change relative to input. **D,** Changes in histone H3K9 -me1, -me2, and -me3 at promoter regions-1 and -2 following DMSO or UNC 0638 treatment (12 hours), were evaluated by ChIP assay. Data is shown as percent fold change relative to input. DAOY cells transduced with a vector control or a plasmid expressing the G9a mutant-G9a^{H1113K} were analyzed by Western blotting to detect global changes in histone H3K9 -me1, -me2, and -me3, with histone H3 serving as a loading control (**E**) and q-RT-PCR to assess expression of known G9a and REST target genes in DAOY cells ectopically expressing mutant G9a^{H1113K} (**F**; *, $P < 0.05$; **, $P < 0.01$; ***, $P < 0.001$; ****, $P < 0.000$, and n.s., not significant).

affected by UNC 0638 treatment compared with DAOY cells at all drug doses and exposure times, which was reflected in higher IC_{50} values of UNC 0638 for DAOY-REST cells relative to DAOY cells (Fig. 4D; Table 2). These observations indicate that elevation of REST protein increases the activity of G9a in complex with REST.

As MTT assay measures relative cell growth, the contribution of cell proliferation, differentiation, or apoptosis to this reduction in cell growth could not be studied. Because *USP37* derepression and p27 stabilization would be expected to lead to terminal G_1 cell-cycle exit/arrest prior to neurogenesis, we also used a DRAQ5 live-cell nuclear staining assay to investigate the effect of G9a inhibition on the cell-cycle transit of DAOY and DAOY-REST cells. Therefore, both cells were treated with DMSO or their respective 48-hour IC_{50} doses of UNC 0638 for 12, 24, or 48 hours, and changes in their DNA contents were followed by flow cytometry. First, although DAOY cells displayed an S–G_2/M–G_1/G_0 cell cycle profile at 12, 24, and 48 hours respectively, DAOY-REST cells exhibited a G_0/G_1/S–S–S/G_2/M/G_1 shift at these time points,

Published OnlineFirst May 8, 2017; DOI: 10.1158/1541-7786.MCR-16-0424

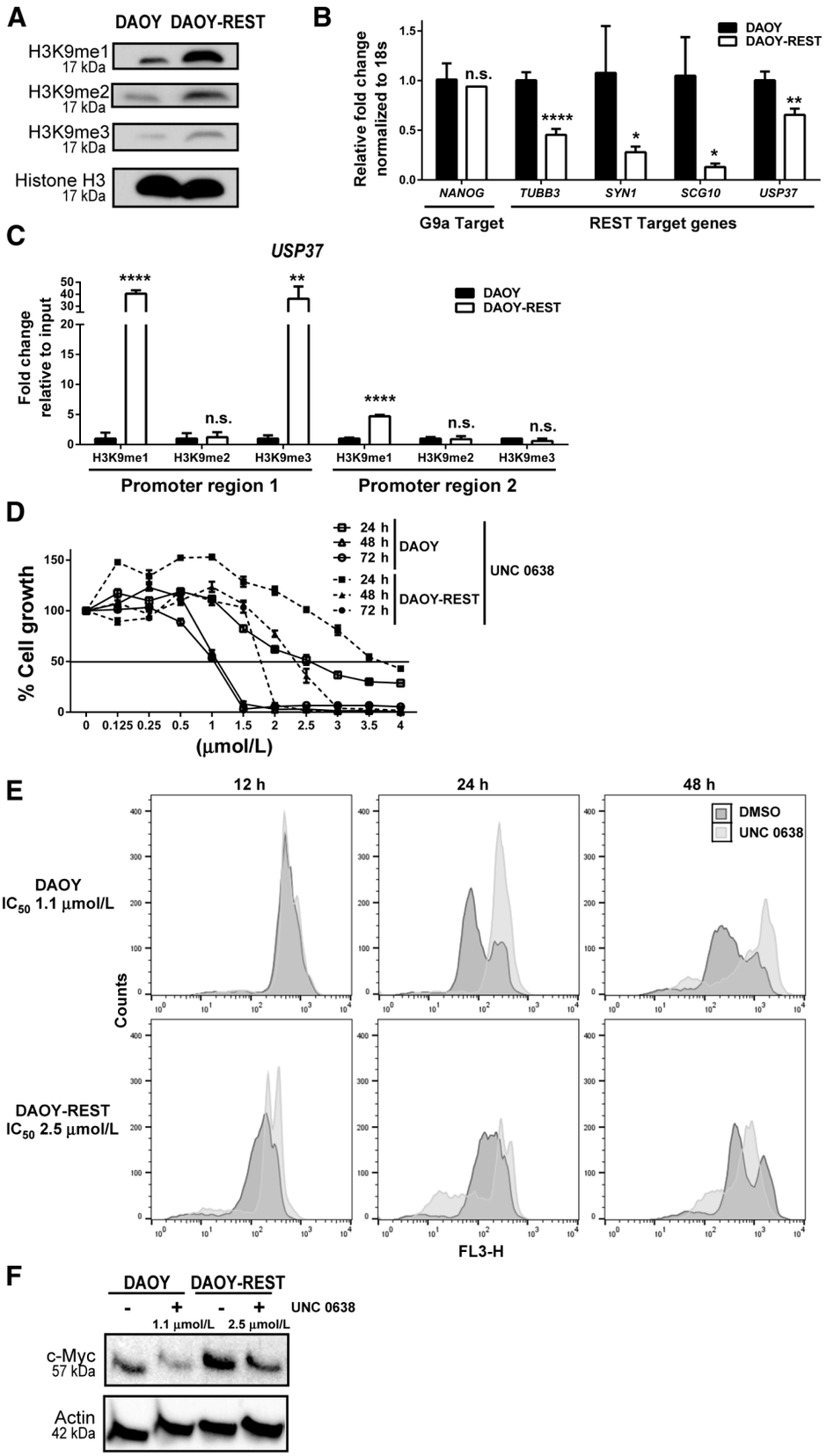

Figure 4.

Elevated REST expression increases G9a-dependent histone methylation and target gene repression. **A,** Western blotting was performed with extracts from isogenic DAOY and DAOY-REST cells to determine the effect of REST elevation on global histone H3K9-me1, -me2, and -me3. Total histone H3 served as the loading control. **B,** Changes in G9a and REST-target gene expression were evaluated by qRT-PCR. **C,** ChIP assay was performed to demonstrate an increase in histone H3K9 -me1 and -me3 at *USP37* promoter region-1 and -me1 at region-2 in DAOY-REST cells relative to DAOY cells. **D,** MTT assays were used to examine the effect of REST elevation in DAOY-REST cells on its response to G9a inhibition compared with DAOY cells. Solid black line, IC_{50} value, which is also tabulated. (*, $P < 0.05$; **, $P < 0.01$; ****, $P < 0.0001$, and n.s., not significant). **E,** Live-cell nuclear staining assay was performed using DRAQ5 to distinguish between cytotoxic and cytostatic effects of UNC 0638 treatment on DAOY and DAOY-REST cells. **F,** Western blotting analysis was performed to measure the levels of the GLP target protein c-Myc following treatment of DAOY and DAOY-REST cells with 48-hour IC_{50} doses of UNC 0638. β-Actin was used as a loading control.

Published OnlineFirst May 8, 2017; DOI: 10.1158/1541-7786.MCR-16-0424

Table 2. Comparison of IC_{50} values of UNC 0638 in low- and high-REST isogenic cells

	IC_{50} Values		
Time (hours)	24	48	72
DAOY (μmol/L)	2.7	1.1	1.1
DAOY-REST (μmol/L)	3.6	2.5	1.8

suggesting that REST elevation causes a delay in cell-cycle transit (Fig. 4E, top and bottom). Second, when compared with control DMSO-treated DAOY cells, UNC 0638-treated cells accumulated with S- and G_2/M/sub-G_1 DNA contents at 24 and 48 hours, respectively, suggesting a cell-cycle delay and possibly arrest at G_2–M, followed by induction of apoptosis in a small fraction of cells (Fig. 4E, top). In contrast, UNC 0638 treatment of DAOY-REST cells revealed transition of cells with a predominantly G_1/G_0/S DNA content at 12 hours to a sub-G_1/G_1/S profile at 24 and 48 hours. A striking difference was the substantial increase in the number of DAOY-REST cells with sub-G_1 DNA content, suggesting that REST elevation sensitizes these cells to apoptosis by UNC 0638 treatment. However, an arrest phenotype seen with a significant number of DAOY and DAOY-REST cells would suggest that the effect of G9a is cytostatic and is consistent with a role for REST in controlling neuronal differentiation.

We next asked whether UNC 0638 treatment affected the activity of G9a-like protein (GLP), a heterodimeric partner for G9a, by measuring levels of its target protein c-Myc by Western blotting. As shown in Fig. 4F, c-Myc levels declined in both DAOY and DAOY-REST cells following exposure to their respective 48-hour IC_{50} concentrations of the drug for 12 hours, indicating that G9a inhibition also affected the activity of GLP in a REST-dependent manner.

Finally, to understand the molecular basis of resistance of DAOY-REST cells to growth inhibition by UNC 0638, these cells were treated with the drug under the same conditions that elicited a derepression of REST target genes in DAOY cells. Despite the global decrease in histone H3K9 -me1, -me2, and -me3, treatment with UNC 0638 failed to upregulate the expression of REST target genes involved in neuronal differentiation (*SYN1*, *TUBB3*, and *SCG10*) and cell-cycle control (*USP37*), although *NANOG* expression was elevated under these conditions (Fig. 5A and B). A decline in c-Myc levels was also not observed following treatment with 1.1 μmol/L UNC 0638 (Fig. 5C). An analysis of histone H3K9 methylation at regions-1 and -2 of *USP37* promoter following drug treatment showed an elevated retention (13.5- to 12.3-fold) of histone H3K9-me1 at regions-1 and -2 in DAOY cells compared with DAOY-REST cells. A 3-fold increased retention of histone H3K9-me3 was also seen at region-2 of the *USP37* promoter, whereas the relative histone H3K9-me2at regions-1 and -2 were significantly lower in DAOY cells when compared with DAOY-REST cells (Fig. 5D). Ectopic expression of the G9a-H1113K mutant in DAOY-REST cells resulted in decreased global histone H3K9-me3 only (Fig. 5E). Under these conditions, expression of *NANOG* and *TUBB3* expression was derepressed, whereas *USP37* and *SCG10* transcripts were unaffected relative to control vector-transfected cells (Fig. 5F). Treatment of DAOY-REST cells with the IC_{50} dose of UNC 0638 used in previous experiments with DAOY cells did not significantly block tumor growth of DAOY-REST cells *in vivo* relative to animals implanted with untreated cells, suggesting that REST elevation associated increase in G9a activity may contribute to the decreased response of cells to UNC 0638 (Fig. 2E and data not shown).

Discussion

The application of next-generation sequencing technologies to the analysis of human medulloblastoma samples has led to the identification of genomic aberrations such as copy number variations and recurrent mutations in these tumors (29–31). This has provided the basis for not only a new molecular classification of medulloblastomas, but also the foundation for functional studies in animal models (32, 33). An interesting outcome of these high-throughput studies is the uncovering of somatic mutations, amplifications, and loss of chromatin-modifying enzymes, implicating epigenetic perturbations in medulloblastoma genesis (34). However, this is an emerging field and the biological consequences of these changes or how these events can be targeted for clinical application remain to be elucidated. Aberrations in post-translational modifications in medulloblastoma and their contribution to tumor development are even less understood, although work in many cancers has highlighted their critical role in oncology. Here, we have focused on dissecting the role of protein ubiquitination and its deregulation in medulloblastoma biology.

In our previous work, we showed that the DUB, USP37, plays a significant role in controlling medulloblastoma cell proliferation and onset of terminal differentiation (5). Work from previous groups has underscored the importance of the CDKI-p27, and its spatial and temporal elevation in granule cell progenitors in coordinating the switch between cell-cycle exit and initiation of neuronal differentiation during normal cerebellar development (35–37). In human medulloblastoma samples, p27 is either expressed at low levels or absent when compared with normal cerebella. The regulation of p27 during normal postnatal cerebellar development and in pathologic conditions, such as medulloblastoma, is not well understood. Our discovery that the down-regulation or loss of USP37 in medulloblastoma cells and the consequent failure to stabilize p27 served to introduce the involvement of DUBs in medulloblastoma etiology (5).

Downregulation of *USP37* and p27 observed in human medulloblastoma tumors and cell lines, as well as the consequent deregulation of proliferation in cell lines, suggests that USP37 may have a tumor-suppressive function in this neural tumor (5). Consistent with this prediction, orthotopic transplantation assays revealed a loss of tumorigenic potential and Ki-67 staining in REST-positive medulloblastoma cells with ectopic *USP37* expression. A similar tumor-suppressive role for USP37 has been suggested by a recent report by Hernandez-Perez and colleagues, who identified the licensing factor Cdt1 as a target of USP37 (38). Cdt1 in concert with Cdc18/CDC6 monitors origin firing and regulates DNA ploidy, and genomic integrity (39, 40). Cdt1 levels are therefore tightly regulated, and its stabilization by USP37 in late G_1 and its degradation in the S-phase likely prevents reinitiation of DNA synthesis from the same origin and within a single cell cycle. USP37 was also recently identified as a facilitator of sister chromatid separation and mitotic progression in an RNAi screen (41). The assumption here would be that its loss during mitosis will lead to improper chromosome segregation and genomic instability.

However, the following studies ascribe an oncogenic role for USP37. USP37 is known to be necessary for the deubiquitination and stabilization of the cell-cycle regulatory protein, cyclin A, which is critical for G_1–S transition in HeLa and U2OS cells (17). The oncogene, c-Myc, is overexpressed in many cancers, including

Published OnlineFirst May 8, 2017; DOI: 10.1158/1541-7786.MCR-16-0424

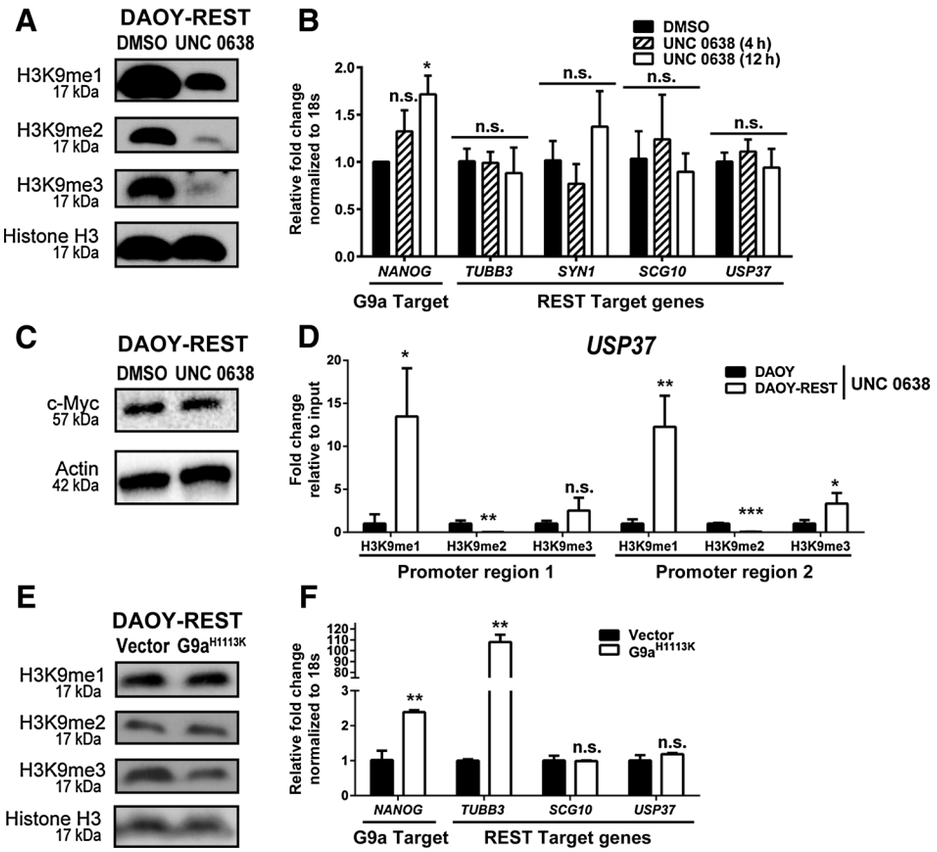

Figure 5.

REST elevation counters derepression of target genes by G9a inhibition. **A,** DAOY-REST cell extracts were subjected to Western blot analyses to measure levels of histone H3K9-me1, -me2, and -me3 following exposure to 1.1 μmol/L UNC 0638 (or DMSO) for 12 hours. Total histone H3 served as the loading control. **B,** Changes in the expression of G9a and REST-target genes in DAOY-REST cells treated with 1.1 μmol/L UNC 0638 was shown by qRT-PCR. **C.** Western blotting analysis was performed to measure the levels of the GLP target protein c-Myc following treatment of DAOY and DAOY-REST cells with a 48-hour IC_{50} dose of UNC 0638 (1.1 μmol/L) for DAOY cells. β-Actin was used as a loading control. **D,** ChIP assays were performed to demonstrate residual histone H3K9-me1, -me2, and -me3 within *USP37* promoter regions-1 and -2 in DAOY-REST cells relative to DAOY cells following drug treatment. Data, fold change relative to input. **E,** Western blotting was performed to assess global changes in G9a-dependent histone H3K9-me1, -me2, and -me3 in DAOY-REST cells transduced with $G9a^{H1113K}$ or vector (control). Histone H3 was used as loading control. **F,** qRT-PCR to assess expression of known G9a and REST-target genes in DAOY-REST cells ectopically expressing mutant $G9a^{H1113K}$ (*, $P < 0.05$; **, $P < 0.01$; ***, $P < 0.001$, and n.s., not significant).

lung cancer, and this elevation occurs in part due its USP37-dependent stabilization (15, 42). The retinoic acid receptor alpha and the promyelocytic leukemia zinc finger (PLZF) fusion protein is a target of USP37, and the stabilization of PLZF and oncogenic transformation of acute promyelocytic leukemia cells has been attributed to USP37 (16). USP37 activity is believed to underlie the overexpression of 14-3-3γ protein and the consequent increase in proliferation of leukemia cells, providing support for an oncogenic role for USP37 (43).

The regulation of USP37 expression and activity involves transcriptional and posttranscriptional mechanisms in nonneural cells such as Hela (17, 44). Our findings described here serve to highlight the contribution of epigenetics to *USP37* regulation in neural cells. *USP37* was identified by our group as a novel target of REST, a major regulator of brain development and neurogenesis, and whose expression is aberrantly elevated in human medulloblastoma tumors (5). REST controls the expression of target genes through one or both of its corepressor complexes and in a context-dependent manner. The failure of the HDAC inhibitor, MS-275, to upregulate *USP37* expression suggests that either HDAC1/2 activities are not necessary or are alone insufficient to derepress *USP37* expression (Fig. 2B).

However, our pharmacologic and genetic data do implicate the Co-REST complex, and specifically G9a, in epigenetic regulation of *USP37* expression. G9a catalyzes mono- and dimethylation of histone H3K9, and its HMT activity correlates with gene repression, which is in agreement with our observations with respect to *USP37* (28, 45, 46). Interestingly, the *USP37* promoter exhibited a significant level of trimethylation of histone H3K9, which was considerably diminished following inhibition of G9a activity by UNC 0638 (Fig. 3D). In support of this, a decrease in histone H3K9 trimethylation has been demonstrated at a subset of G9a target genes in cells treated with the G9a inhibitor, BIX-01294 (47). Although a direct role for G9a in promoting histone H3K9 trimethylation cannot be excluded in our studies, G9a is known to exist in a complex with histone H3K9 trimethylases Suv39H1 and

Published OnlineFirst May 8, 2017; DOI: 10.1158/1541-7786.MCR-16-0424

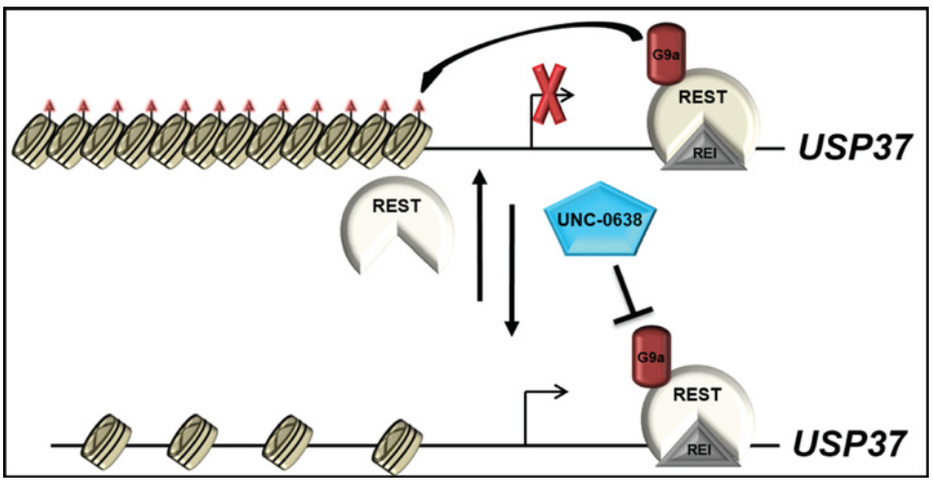

Figure 6.

Model to summarize the effect of G9a inhibition on *USP37* gene expression. REST and its associated chromatin remodelers, including G9a, bind to a *RE1*-binding site in exon 1 of *USP37* gene and repress its expression by di- and trimethylation of histone H3K9 (orange triangles). From previous studies, USP37 is a p27-specific deubiquitylase, and its loss in REST-expressing medulloblastoma cells leads to p27 degradation and sustained proliferation. Inhibition of REST-associated G9a enzymatic activity by UNC 0638 derepresses *USP37* gene expression by blocking histone H3K9 methylation at its promoter, causes an increase in p27 levels, and promotes a blockade of tumor growth in mouse intracranial models.

SETDB1 and its heterodimeric partner GLP, in the context of specific genes (48). It is also well established that the activity of these trimethylases can affect the expression of G9a target genes (48). Thus, a function link between G9a and these proteins at the *USP37* promoter could potentially explain the observed elevation in histone H3K9 trimethylation.

A second point of interest stems from our findings of a REST-dependent global increase in G9a-dependent histone H3K9 mono- and di- and trimethylation as well as an augmentation of histone H3K9 mono- and trimethylation at the *USP37* promoter. A role for the zinc finger binding protein, WIZ, in the retention of G9a on chromatin has been suggested by a recent study by Simon and colleagues (49). Whether REST, also a zinc finger protein, promotes a similar retention of G9a at genes with *RE1* elements remains to be evaluated. In this regard, it is important to note that *WIZ* isoforms are highly expressed in the cerebellum, and medulloblastoma is a disease of cerebellar origins (50). The G9a/GLP complex has been implicated in the regulation of c-Myc protein (51). The REST-dependent increase in GLP activity as measured by a decline in c-Myc protein levels in DAOY cells (Figs. 4F and 5C) not only connects REST to the G9a partner-GLP, but also provides the first link between REST and c-Myc, which are often coelevated in human medulloblastoma (6).

In summary, our study is the first to implicate G9a-dependent chromatin remodeling in the control of *USP37* expression (Fig. 6). Blockade of G9a activity reactivates *USP37* expression, which we previously showed as being necessary for stabilization of p27 and cessation of medulloblastoma cell proliferation, and impeded their tumorigenic potential *in vivo* (Fig. 6). We therefore suggest that G9a inhibitors may have therapeutic application, which warrants further evaluation in patient-derived xenograft models.

Disclosure of Potential Conflicts of Interest

No potential conflicts of interest were disclosed.

Authors' Contributions

Conception and design: J. Swaminathan, R.-H. Tao, P.H. Taylor, V. Gopalakrishnan

Development of methodology: J. Swaminathan, C.M. Das, R.-H. Tao, P.H. Taylor

Acquisition of data (provided animals, acquired and managed patients, provided facilities, etc.): T.H.W. Dobson, J. Swaminathan, C.M. Das, R.-H. Tao, V. Gopalakrishnan

Analysis and interpretation of data (e.g., statistical analysis, biostatistics, computational analysis): T.H.W. Dobson, R.J. Hatcher, J. Swaminathan, R.-H. Tao, P.H. Taylor, V. Gopalakrishnan

Writing, review, and/or revision of the manuscript: T.H.W. Dobson, R.J. Hatcher, J. Swaminathan, R.-H. Tao, G. Sbardella, V. Gopalakrishnan

Administrative, technical, or material support (i.e., reporting or organizing data, constructing databases): T.H.W. Dobson, R.J. Hatcher, V. Gopalakrishnan

Study supervision: T.H.W. Dobson, R.J. Hatcher, V. Gopalakrishnan

Other (contributed to *in vitro* studies and Western blot analysis): S. Shaik

Other (synthesis of reagents): C. Milite, S. Castellano

Other (supervision of the medicinal chemistry part): G. Sbardella

Acknowledgments

The authors thank Dr. Xiaobing Shi for providing reagents and Dr. Mark Bedford for helpful comments.

Grant Support

This work was supported by grants from the NIH (5R01-NS-079715-01), American Cancer Society (RSG-09-273-01-DDC) and Cancer Prevention Research Institute of Texas (CPRIT-RP150301) to V. Gopalakrishnan, The UT MD Anderson Cancer Center-CCE Scholar Program (to T.H.W. Dobson), and Cancer Center support grant NCI#CA16672 (to the Characterized Cell Line Core).

The costs of publication of this article were defrayed in part by the payment of page charges. This article must therefore be hereby marked *advertisement* in accordance with 18 U.S.C. Section 1734 solely to indicate this fact.

Received November 23, 2016; revised March 16, 2017; accepted May 2, 2017; published OnlineFirst May 8, 2017.

References

1. Kool M, Korshunov A, Remke M, Jones DT, Schlanstein M, Northcott PA, et al. Molecular subgroups of medulloblastoma: an international meta-analysis of transcriptome, genetic aberrations, and clinical data of WNT, SHH, Group 3, and Group 4 medulloblastomas. Acta Neuropathol 2012;123:473–84.
2. Rusert JM, Wu X, Eberhart CG, Taylor MD, Wechsler-Reya RJ. SnapShot: medulloblastoma. Cancer Cell 2014;26:940–e1.
3. Taylor MD, Northcott PA, Korshunov A, Remke M, Cho YJ, Clifford SC, et al. Molecular subgroups of medulloblastoma: the current consensus. Acta Neuropathol 2012;123:465–72.
4. Coluccia D, Figuereido C, Isik S, Smith C, Rutka JT. Medulloblastoma: tumor biology and relevance to treatment and prognosis paradigm. Curr Neurol Neurosci Rep 2016;16:43.
5. Das CM, Taylor P, Gireud M, Singh A, Lee D, Fuller G, et al. The deubiquitylase USP37 links REST to the control of p27 stability and cell proliferation. Oncogene 2013;32:1691–701.
6. Su X, Gopalakrishnan V, Stearns D, Aldape K, Lang FF, Fuller G, et al. Abnormal expression of REST/NRSF and Myc in neural stem/progenitor cells causes cerebellar tumors by blocking neuronal differentiation. Mol Cell Biol 2006;26:1666–78.
7. Taylor P, Fangusaro J, Rajaram V, Goldman S, Helenowski IB, MacDonald T, et al. REST is a novel prognostic factor and therapeutic target for medulloblastoma. Mol Cancer Ther 2012;11:1713–23.
8. Lawinger P, Venugopal R, Guo ZS, Immaneni A, Sengupta D, Lu W, et al. The neuronal repressor REST/NRSF is an essential regulator in medulloblastoma cells. Nat Med 2000;6:826–31.
9. Chen ZF, Paquette AJ, Anderson DJ. NRSF/REST is required in vivo for repression of multiple neuronal target genes during embryogenesis. Nat Genet 1998;20:136–42.
10. Chong JA, Tapia-Ramirez J, Kim S, Toledo-Aral JJ, Zheng Y, Boutros MC, et al. REST: a mammalian silencer protein that restricts sodium channel gene expression to neurons. Cell 1995;80:949–57.
11. McGann JC, Oyer JA, Garg S, Yao H, Liu J, Feng X, et al. Polycomb- and REST-associated histone deacetylases are independent pathways toward a mature neuronal phenotype. eLife 2014;3:e04235.
12. Canzonetta C, Mulligan C, Deutsch S, Ruf S, O'Doherty A, Lyle R, et al. DYRK1A-dosage imbalance perturbs NRSF/REST levels, deregulating pluripotency and embryonic stem cell fate in Down syndrome. Am J Hum Genet 2008;83:388–400.
13. Clague MJ, Barsukov I, Coulson JM, Liu H, Rigden DJ, Urbe S. Deubiquitylases from genes to organism. Physiol Rev 2013;93:1289–315.
14. Jara JH, Frank DD, Ozdinler PH. Could dysregulation of UPS be a common underlying mechanism for cancer and neurodegeneration? Lessons from UCHL1. Cell Biochem Biophys 2013;67:45–53.
15. Pan J, Deng Q, Jiang C, Wang X, Niu T, Li H, et al. USP37 directly deubiquitinates and stabilizes c-Myc in lung cancer. Oncogene 2015;34:3957–67.
16. Yang WC, Shih HM. The deubiquitinating enzyme USP37 regulates the oncogenic fusion protein PLZF/RARA stability. Oncogene 2013;32:5167–75.
17. Huang X, Summers MK, Pham V, Lill JR, Liu J, Lee G, et al. Deubiquitinase USP37 is activated by CDK2 to antagonize APC(CDH1) and promote S phase entry. Mol Cell 2011;42:511–23.
18. Deshaies RJ, Joazeiro CA. RING domain E3 ubiquitin ligases. Annu Rev Biochem 2009;78:399–434.
19. Nijman SM, Luna-Vargas MP, Velds A, Brummelkamp TR, Dirac AM, Sixma TK, et al. A genomic and functional inventory of deubiquitinating enzymes. Cell 2005;123:773–86.
20. Barakat K, Tuszynski J. Relaxed complex scheme suggests novel inhibitors for the lyase activity of DNA polymerase beta. J Mol Graph Model 2011;29:702–16.
21. D'Arcy P, Linder S. Proteasome deubiquitinases as novel targets for cancer therapy. Int J Biochem Cell Biol 2012;44:1729–38.
22. Chang Y, Ganesh T, Horton JR, Spannhoff A, Liu J, Sun A, et al. Adding a lysine mimic in the design of potent inhibitors of histone lysine methyltransferases. J Mol Biol 2010;400:1–7.
23. Vedadi M, Barsyte-Lovejoy D, Liu F, Rival-Gervier S, Allali-Hassani A, Labrie V, et al. A chemical probe selectively inhibits G9a and GLP methyltransferase activity in cells. Nat Chem Biol 2011;7:566–74.
24. Lal S, Lacroix M, Tofilon P, Fuller GN, Sawaya R, Lang FF. An implantable guide-screw system for brain tumor studies in small animals. J Neurosurg 2000;92:326–33.
25. Nomura M, Uda-Tochio H, Murai K, Mori N, Nishimura Y. The neural repressor NRSF/REST binds the PAH1 domain of the Sin3 corepressor by using its distinct short hydrophobic helix. J Mol Biol 2005;354:903–15.
26. Stewart MD, Li J, Wong J. Relationship between histone H3 lysine 9 methylation, transcription repression, and heterochromatin protein 1 recruitment. Mol Cell Biol 2005;25:2525–38.
27. Lee DY, Northrop JP, Kuo MH, Stallcup MR. Histone H3 lysine 9 methyltransferase G9a is a transcriptional coactivator for nuclear receptors. J Biol Chem 2006;281:8476–85.
28. Tachibana M, Sugimoto K, Fukushima T, Shinkai Y. Set domain-containing protein, G9a, is a novel lysine-preferring mammalian histone methyltransferase with hyperactivity and specific selectivity to lysines 9 and 27 of histone H3. J Biol Chem 2001;276:25309–17.
29. Mendrzyk F, Radlwimmer B, Joos S, Kokocinski F, Benner A, Stange DE, et al. Genomic and protein expression profiling identifies CDK6 as novel independent prognostic marker in medulloblastoma. J Clin Oncol 2005;23:8853–62.
30. Northcott PA, Nakahara Y, Wu X, Feuk L, Ellison DW, Croul S, et al. Multiple recurrent genetic events converge on control of histone lysine methylation in medulloblastoma. Nat Genet 2009;41:465–72.
31. Parsons DW, Li M, Zhang X, Jones S, Leary RJ, Lin JC, et al. The genetic landscape of the childhood cancer medulloblastoma. Science 2011;331:435–9.
32. Ecke I, Petry F, Rosenberger A, Tauber S, Monkemeyer S, Hess I, et al. Antitumor effects of a combined 5-aza-2'deoxycytidine and valproic acid treatment on rhabdomyosarcoma and medulloblastoma in Ptch mutant mice. Cancer Res 2009;69:887–95.
33. Patties I, Kortmann RD, Glasow A. Inhibitory effects of epigenetic modulators and differentiation inducers on human medulloblastoma cell lines. J Exp Clin Cancer Res 2013;32:27.
34. Jones DT, Northcott PA, Kool M, Pfister SM. The role of chromatin remodeling in medulloblastoma. Brain Pathol 2013;23:193–9.
35. Ayrault O, Zindy F, Rehg J, Sherr CJ, Roussel MF. Two tumor suppressors, p27Kip1 and patched-1, collaborate to prevent medulloblastoma. Mol Cancer Res 2009;7:33–40.
36. Bhatia B, Northcott PA, Hambardzumyan D, Govindarajan B, Brat DJ, Arbiser JL, et al. Tuberous sclerosis complex suppression in cerebellar development and medulloblastoma: separate regulation of mammalian target of rapamycin activity and p27 Kip1 localization. Cancer Res 2009;69:7224–34.
37. Zindy F, Knoepfler PS, Xie S, Sherr CJ, Eisenman RN, Roussel MF. N-Myc and the cyclin-dependent kinase inhibitors p18Ink4c and p27Kip1 coordinately regulate cerebellar development. Proc Natl Acad Sci U S A 2006;103:11579–83.
38. Hernandez-Perez S, Cabrera E, Amoedo H, Rodriguez-Acebes S, Koundrioukoff S, Debatisse M, et al. USP37 deubiquitinates Cdt1 and contributes to regulate DNA replication. Mol Oncol 2016;10:1196–206.
39. Brown GW, Jallepalli PV, Huneycutt BJ, Kelly TJ. Interaction of the S phase regulator cdc18 with cyclin-dependent kinase in fission yeast. Proc Natl Acad Sci U S A 1997;94:6142–7.
40. Gopalakrishnan V, Simancek P, Houchens C, Snaith HA, Frattini MG, Sazer S, et al. Redundant control of rereplication in fission yeast. Proc Natl Acad Sci U S A 2001;98:13114–9.
41. Yeh C, Coyaud E, Bashkurov M, van der Lelij P, Cheung SW, Peters JM, et al. The deubiquitinase USP37 regulates chromosome cohesion and mitotic progression. Curr Biol 2015;25:2290–9.
42. Sun XX, Sears RC, Dai MS. Deubiquitinating c-Myc: USP36 steps up in the nucleolus. Cell Cycle 2015;14:3786–93.
43. Kim JO, Kim SR, Lim KH, Kim JH, Ajjappala B, Lee HJ, et al. Deubiquitinating enzyme USP37 regulating oncogenic function of 14-3-3gamma. Oncotarget 2015;6:36551–76.
44. Burrows AC, Prokop J, Summers MK. Skp1-Cul1-F-box ubiquitin ligase (SCF(betaTrCP))-mediated destruction of the ubiquitin-specific protease USP37 during G2-phase promotes mitotic entry. J Biol Chem 2012;287:39021–9.

Published OnlineFirst May 8, 2017; DOI: 10.1158/1541-7786.MCR-16-0424

45. Mozzetta C, Boyarchuk E, Pontis J, Ait-Si-Ali S. Sound of silence: the properties and functions of repressive Lys methyltransferases. Nat Rev Mol Cell Biol 2015;16:499–513.
46. Shankar SR, Bahirvani AG, Rao VK, Bharathy N, Ow JR, Taneja R. G9a, a multipotent regulator of gene expression. Epigenetics 2013;8:16–22.
47. Kubicek S, O'Sullivan RJ, August EM, Hickey ER, Zhang Q, Teodoro ML, et al. Reversal of H3K9me2 by a small-molecule inhibitor for the G9a histone methyltransferase. Mol Cell 2007;25:473–81.
48. Fritsch L, Robin P, Mathieu JR, Souidi M, Hinaux H, Rougeulle C, et al. A subset of the histone H3 lysine 9 methyltransferases Suv39h1, G9a, GLP, and SETDB1 participate in a multimeric complex. Mol Cell 2010;37:46–56.
49. Simon JM, Parker JS, Liu F, Rothbart SB, Ait-Si-Ali S, Strahl BD, et al. A role for widely interspaced zinc finger (WIZ) in retention of the G9a methyltransferase on chromatin. J Biol Chem 2015;290:26088–102.
50. Matsumoto K, Ishii N, Yoshida S, Shiosaka S, Wanaka A, Tohyama M. Molecular cloning and distinct developmental expression pattern of spliced forms of a novel zinc finger gene wiz in the mouse cerebellum. Brain Res Mol Brain Res 1998;61:179–89.
51. Liu C, Yu Y, Liu F, Wei X, Wrobel JA, Gunawardena HP, et al. A chromatin activity-based chemoproteomic approach reveals a transcriptional repressome for gene-specific silencing. Nat Commun 2014;5:5733.

AACR American Association for Cancer Research

Molecular Cancer Research

Regulation of *USP37* Expression by REST-Associated G9a-Dependent Histone Methylation

Tara H.W. Dobson, Rashieda J. Hatcher, Jyothishmathi Swaminathan, et al.

Mol Cancer Res 2017;15:1073-1084. Published OnlineFirst May 8, 2017.